THERMOELECTRIC POWER FOR LIQUID Tl-S ALLOYS CORRELATED TO THE PHASE DIAGRAM

Ştefan Alexandru ADAM[1], Mihai BUZATU[2], Mircea Ionuț PETRESCU[3]

The thermoelectric power was measured in three liquid Tl-S alloys (54; 50 and 45at.%Tl) in a temperature range including the pre-freezing region. For all alloys a dual behavior was identified in the Seebeck coefficient dependence on temperature. In the high temperature range the behavior was similar to the one obtained in a previous research for liquid alloys richer in thallium (57.1 and 64.7at.%Tl), namely decrease of the Seebeck coefficient as the temperature increases (a typical behavior for a one band semiconductor). In the low temperature range down to the liquidus point, a different behavior was manifest, namely increase of the Seebeck coefficient as the temperature increases. The overheating range above the liquidus point in which this second type of behaviour was noticed became broader as the Tl content decreased. The two types of behavior have been associated with the phase transformations that take place during heating in view of melting, more specifically with the nature of the last crystals to dissolve in the melt. The nature of these crystals was different in the alloys exhibiting a unique semiconductor behavior (Tl_2S crystals) and in alloys exhibiting a dual behavior (Tl_4S_3 or TlS crystals).

Keywords: liquid Tl-S alloys, thermoelectric power, pre-freezing range, phase diagram

1. Introduction

The interest in liquid semiconductors as thermoelectric materials for the direct conversion of thermal energy in electricity is related to their convenient thermoelectrical power and electrical conductivity coupled with low phononic thermal conductivity κ_{ph}, the latter beeing appreciable smaller than in crystalline solids at the same temperature. So large values for the figure of merit $ZT(=\sigma S^2T/\kappa)$ can be obtained (where σ=electrical conductivity, S=Seebeck coefficient and $\kappa=\kappa_{ph},+ \kappa_{el}$ =toyal thermal conductivity). Also important is the fact that the liquid structure is not affected by structural transformations induced by electromagnetic radiations (radiation damage) as it happens in the solid structure.

[1] Ph.D Student, Faculty of Materials Science and Engineering University POLITEHNICA of Bucharest, ROMANIA, e-mail: adamstefan2003@yahoo.com
[2] Professor, Faculty of Materials Science and Engineering University POLITEHNICA of Bucharest, ROMANIA, e-mail: buzatu.mihai @yahoo.com
[3] Professor, Faculty of Materials Science and Engineering University POLITEHNICA of Bucharest, ROMANIA, e-mail: ipetrescu@yahoo.com

Experimental research on the thermoelectric power of liquid semiconductors manifested a burst in the years 70' and the results were summarized in a series of monographs [1-4]. A reborn interest for thermoelectric materials both in solid state as well as in liquid state became manifest around and beyond year 2000 as a result of an increasing preoccupation towards green energy production as well as microelectronic nano-size power generation and cooling systems [5-9]. This paper presents the results on the thermoelectric power in liquid Tl-S alloys poorer in thallium than the ones we have investigated in previous papers [10,11]. The results of the investigations carried out in this paper have been correlated to the the structure of the last crystals to dissolve in the melt that may have a hereditary influence on the nature of the clusters existing in the melt at low temperature in the pre-freezing range.

2. Experimental

According to ec.(1) the Seebeck coefficient S is defined as the ratio between the thermoelectric power ΔE and the temperature gradient ΔT that has generated it:

$$\Delta E/\Delta T = S\ (\mu V/^{o}C) \tag{1}$$

This relationship is valid in experimental runs carried out at small temperature gradients as the ones used in this research. The proposed temperature for Seebeck coefficient measurement in our experiments was located midway within each temperature gradient. At least four temperature gradients at each temperature at which we intended to determine the Seebeck coefficient (for instance 5^{O}C, 10^{O}C, 15^{O}C, 20^{O}C or almost so) were used. According to ec.(1) the Seebeck coefficient is the slope of the experimental straight line ΔE versus ΔT.

For a full description of the apparatus built for measuring the thermoelectric power in Tl-S liquid alloys the reader is referred to our previous paper [11]. The investigated alloy was introduced in a U-shaped quartz cell set in vertical position in an electric furnace. After attaining the desired temperature, the liquid alloy in one of the columns of the U-shaped cell was slightly overheated by means of an additional heating coil in order to create a small temperature gradient ΔT required for generating the thermoelectric power ΔE. The thermoelectric power was measured between two molybdenum electrodes immersed each one in a column of liquid alloy. The temperature in the two columns of liquid alloy was measured by two thermocouples equally immersed in the liquid. The thermoelectric power between the Mo electrodes as well as the thermoelectric power of the thermocouples was measured by a high precision compensation method coupled to a high precision galvanometer. The atmosphere in the quartz

cell containing the liquid alloy consisted of argon. The alloys were prepared from pure elements (Tl and S) under argon atmosphere in a sealed vial.

3. Results

Three liquid alloys with a high excess of sulfur as compared to the semiconductor Tl_2S compound have been investigated and attested to exhibit a change in the thermoelectric power behavior in the pre-freezing range. The compositions in at.% were as follows: - alloy I: 54 %Tl + 46% S (12.7 % S in excess as compared to the semiconductor compound Tl_2S); - alloy II: 50 %Tl + 50%S (16.7 %S in excess as compared to the compound Tl_2S); - alloy III: 45 %Tl + 55%S (21 at.%S in excess as compared to the compound Tl_2S).

For alloy I (composition 54 at.%Tl +46 at.%S) the thermoelectric power was investigated at four temperatures in liquid state (349.7°C; 401.5°C; 460.2°C; 500.5°C) going down as close as possible to the liquidus point (T_{liq}=340 °C).

The results are given in Fig.1 and Table 1. According to ec.(1) the Seebeck coefficient at each investigated temperature was determined as the slope of the straight line in each graph in Fig.1. It is worth to mention that the correlation coefficient for each best fit straight line was r^2 >0.999.

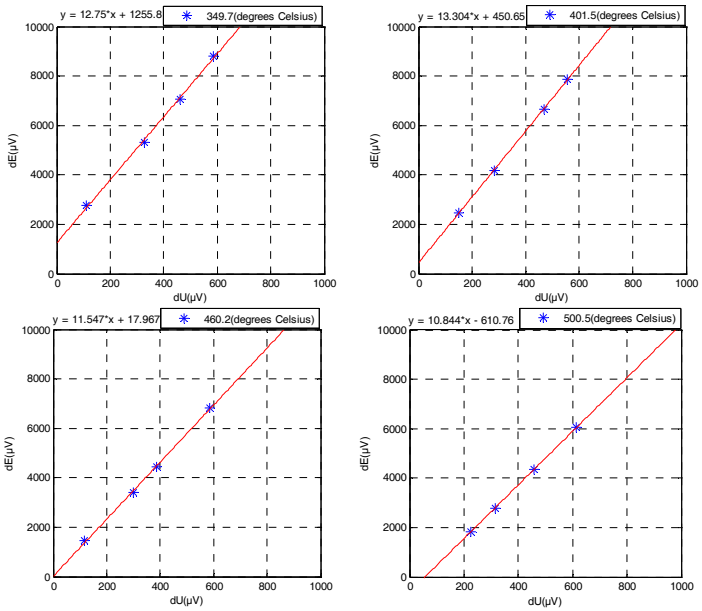

Fig.1 Thermoelectric power dependence on the temperature gradient at various temperatures for alloy I

For a better accuracy the temperature gradient ΔU on the abscissa of each graph in Fig.1 was expressed in μV as indicated directly by the thermocouples. In

this way for obtaining the Seebeck coefficient expressed in μV/^{o}C a single transformation was applied consisting in the multiplication of each slope by a parameter ε that helps to transform the thermoelectric power of the thermocouples from μV into ^{o}C. This parameter ε was calculated at the temperature of each measurement by using the equation specific for the Ni-NiCr thermocouple used in the experiments. Table 1 summarizes the experimental results obtained at the four temperatures investigated for molten alloy I. Also indicated in Table 1 are the steps taken to calculate the absolute Seebeck coefficient S_a of the liquid alloy at each temperature T. It is worth to mention that what we have actually measured was a relative Seebeck coefficient S_{ab} which is the difference between the absolute Seebeck coefficient S_a of the liquid alloy and the absolute Seebeck coefficient S_b of the solid molybdenum electrode:

$$S_{ab} = S_a - S_b \quad (2)$$

For the absolute Seebeck coefficient S_b of solid Mo we have considered in Table 1 the values published by Kusack & Kendall [12] since they have the advantage to cover the low temperature range (<700^{o}C) in which we were interested.

Table 1

Calculation of the absolute Seebeck coefficient from experimental data for molten alloy I (54 at.%Tl + 46 at.%S; 12.7 at.%S in excess as compared with Tl_2S); T_{liq}=340 ^{o}C

T (^{O}C)	ΔT (^{O}C)	ΔU(μV)	ΔE(μV)	ΔE =a ΔU+b	ε	S_{ab} (μV/^{O}C)	S_b (μV/^{O}C)	S_a (μV/^{O}C)
349.7	9.7	111 329 460 584	2755 5320 7070 8800	a= 12.7504 b = 1255.8	29.4213	375.13	14.16	389.29
401.5	61.5	151 282 469 555	2478 4185 6658 7865	a = 13.3036 b = 450.65	29.7345	395.57	14.97	410.54
460.2	120.2	118 300 386 585	1448 3392 4446 6825	a = 11.5473 b = 17.96	30.0894	347.45	15.71	363.16
500.5	160.5	224 316 459 613	1843 2793 4349 6053	a = 10.8443 b = -610.76	30.3331	328.94	16.10	345.04

The meaning of the values in the columns of Table 1 is as follows: T= temperature at which the Seebeck coefficient was measured; ΔT=T-T_{liq}= overheating of the melt above the alloy liquidus temperature; ΔU=difference between the thermoelectric power recorded by the two thermocouples at each thermal gradient; ΔE=thermoelectric power recorded between the two Mo electrodes at each thermal gradient; equation of the straight line in each graph in

Fig.1; ε=factor for transforming the slope of the straight line in μV/^{o}C; S_{ab}=relative Seebeck coefficient of the liquid alloy at temperature T; S_b=absolute Seebeck coefficient of solid molybdenum at temperature T; S_a= absolute Seebeck coefficient of the liquid alloy at temperature T.

For alloy II (composition 50 at.%Tl +50 at.%S) the thermoelectric power in liquid state was investigated at five temperatures (303.2^{o}C; 350.5^{o}C; 401.5^{o}C; 461.5^{o}C; 503.5^{o}C) going down as close as possible to the liquidus point (T_{liq}=295^{O}C). The determination was carried out by using the same procedure as for alloy I. The meaning of the values in the columns of Table 2 is the same as in Table1. The results are given in Fig.2 and in Table 2.

Table 2

Calculation of the absolute Seebeck coefficient from experimental data for molten alloy II (50 at.%Tl + 50 at.%S; 16.7 at.%S in excess as compared with Tl_2S); T_{liq}=295^{O}C)

T (^{O}C)	ΔT (^{O}C)	ΔU (μV)	ΔE (μV)	ΔE =aΔU+b	ε	S_{ab} (μV/^{O}C)	S_b (μV/^{O}C)	S_a (μV/^{O}C)
303.2	8.2	330 363 549 647	10350 10610 12688 13727	a = 10.8044 b = 6741.4	29.1401	314.84	13.31	328.5
350.5	55.5	196 234 405 591	9740 10184 12454 14930	a = 13.1924 b = 7123.9	29.4261	388.20	14.17	402.37
401.5	106.5	63 356 445 586	5422 9146 10051 12136	a = 12.6843 b = 4590.7	29.7345	377.16	14.97	392.13
461.5	166.5	63 293 408 544	3993 6833 8148 9654	a = 11.7944 b = 3300.2	30.0973	354.98	15.73	370.69
503.5	208.5	82 210 335 478	3314 4570 5825 7458	a = 10.4358 b = 2408.9	30.3512	316.74	16.13	332.85

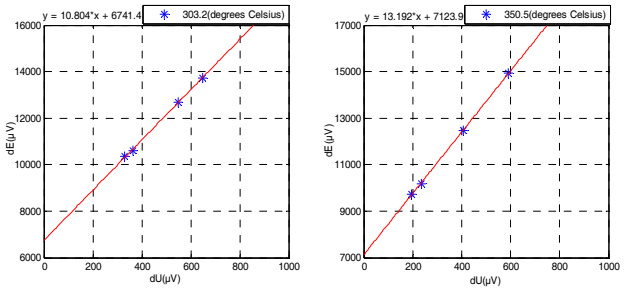

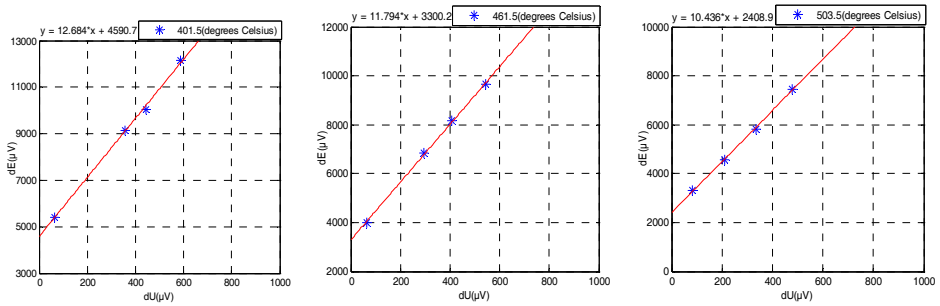

Fig.2 Thermoelectric power dependence on the temperature gradient at various temperatures for alloy II

For alloy III (composition 45 %Tl + 55%S) the values of the Seebeck coefficient S in liquid state were determined at six temperatures (269°C; 306°C; 355°C; 400.2°C; 457°C; 501.75 °C) going down as close as possible to the liquidus point (T_{liq}=265°C). The results are given in Fig.3 and in Table 3.

Table 3

Calculation of the absolute Seebeck coefficient from experimental data for molten alloy III (45 at.%Tl + 55 at.%S; 21.7 at.%S in excess as compared with Tl_2S); (T_{liq}=265°C)

T (°C)	ΔT (°C)	ΔU (μV)	ΔE (μV)	ΔE =aΔU+b	ε	S_{ab} (μV/°C)	S_b (μV/°C)	S_a (μV/°C)
269	4	245 316 463 561	3345 4046 5336 6251	a = 9.1178 b = 1131.6	28.9333	263.80	12,64	276.42
306	41	132 325 451 537	3972 5585 6810 7637	a = 9.0544 b = 2730.1	29.1571	263.99	13.36	277.35
355	90	101 236 459 579	1599 2995 5587 6979	a = 11.3166 b = 399.93	29.4533	333.31	14.25	347.55
400.2	135.2	183 315 428 535	2419 4138 5510 6825	a = 12.4904 b = 160.89	29.7266	371.29	14.95	386.24
457	192	150 221 376 551	2020 2821 4581 6440	a = 11.0403 b = 382.93	30.0701	331.98	15.68	347.65
500.75	235.75	60 276 468 544	850 2806 4718 5460	a = 9.5519 b = 239.50	30.3407	289.81	16.11	305.92

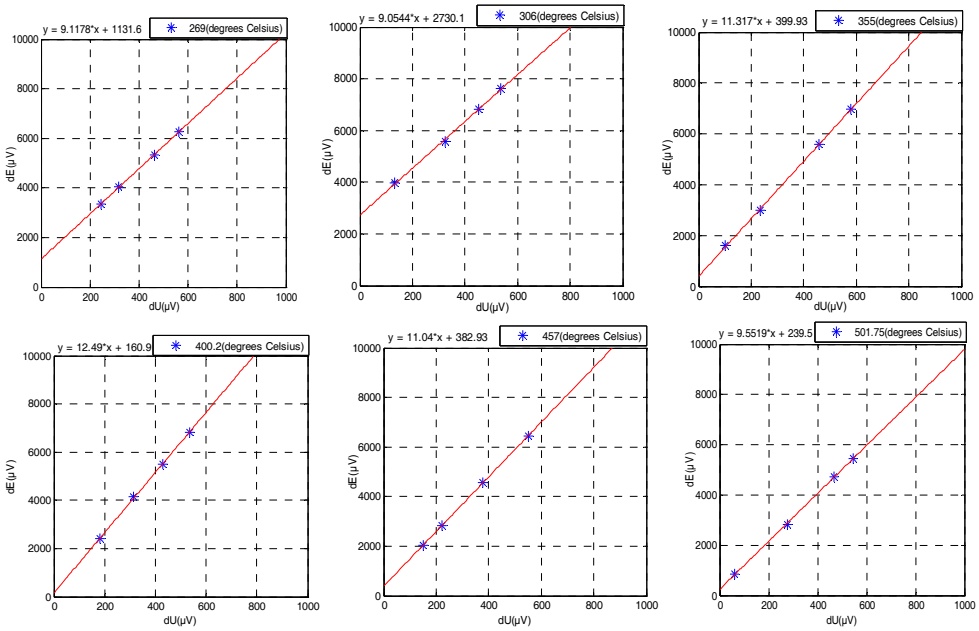

Fig.3 Thermoelectric power dependence on the temperature gradient at various temperatures for alloy III

4. Discussion

A. Dual behavior of the thermoelectric power in function of temperature

In order to make clear the type of behavior of the absolute Seebeck coefficient in the melt we have represented in Fig.4a and Fig.4b the experimental data summarized in Tables 1, 2 and 3. In Fig.4a we have considered temperature as the independent variable, while in Fig.4b we have put on the abscissa the overheating of the melt above the liquidus point of each alloy. The advantage of using the overheating instead of temperature appears obvious in Fig.4b where it is clearly seen that for all three alloys we have encompassed the pre-freezing range (the lowest investigated temperature being close to the liquidus point). Generally speaking, in our opinion it is more meaningful to use the overheating of the melt because it indicates how far apart the melt is from the moment when the alloy has become completely liquid.

Figures 4a and 4b show that for all three molten alloys the temperature dependence of the Seebeck coefficient is different in the high temperature range and in the low temperature range (the latter encompassing the pre-freezing range).

In the high temperature range the behavior is similar to the one we have obtained in a previous paper [11] for molten Tl-S alloys richer in thallium, namely decrease of the Seebeck coefficient as the temperature increases. Such a behavior specific for a one band semiconductor substance is no more observed in the low

temperature range in Fig.4a and 4b where the Seebeck coefficient increases as the temperature increases. This second type of behavior is rather a metallic behavior.

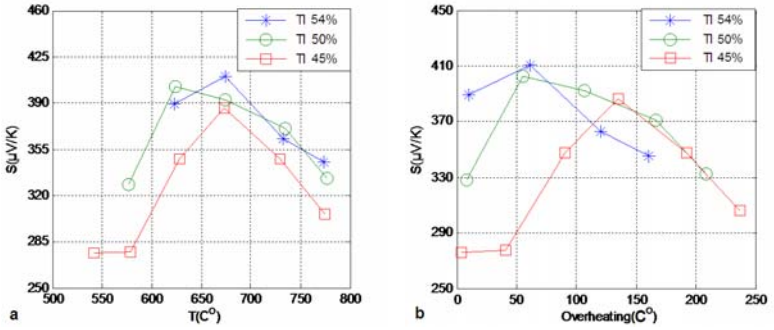

Fig.4 Absolute Seebeck coefficient of the melt for the investigated Tl-S alloys: a. plotted versus temperature; b. plotted versus overheating of the melt above the liquidus point

Such a dual behavior has not been remarked by previous researchers who have investigated the thermoelectric power in liquid alloys belonging to the Tl-S system. These researches have been performed years ago [13,14] at temperatures far above the liquidus point. A simple inspection of the isotherms of the thermoelectric power in liquid Tl-S alloys reproduced by Cutler [3] from the paper of Kazandzhan & A.A.Tsurikov [14(d)] shows that the lowest temperature investigated by these authors was 427^{O}C. By comparison with our experimental data in Fig.4a it appears obvious that such a temperature is out of the range in which we have noticed an anomalous behavior of the Seebeck coefficient.

In terms of overheating of the melt (Fig.4b), the temperature range in which this second type of behavior is manifest (increase of the Seebeck coefficient when increasing the temperature) is as folows: 0- 61.5 ^{O}C overheating above the liquidus for alloy I (54at.%Tl); 0-55^{O}C overheating above the liquidus for alloy II (50at.%Tl); 0-135 ^{O}C overheating above the liquidus for alloy III (45 at.%Tl). As seen this temperature range becomes broader as the sulfur content increases. From an experimental point of view the wider overheating range for alloy III has made possible to obtain a larger number of experimental points.

B. Correlation of the experimental data with the information from the phase diagram

Fig.5 presents the form of the Tl-S system phase diagram published by Massalski et al. [15] in an international handbook ASM. Recently a new form of the Tl-S phase equilibrium diagram (Fig.6) has been published by Vassiliev and Minaev[16].

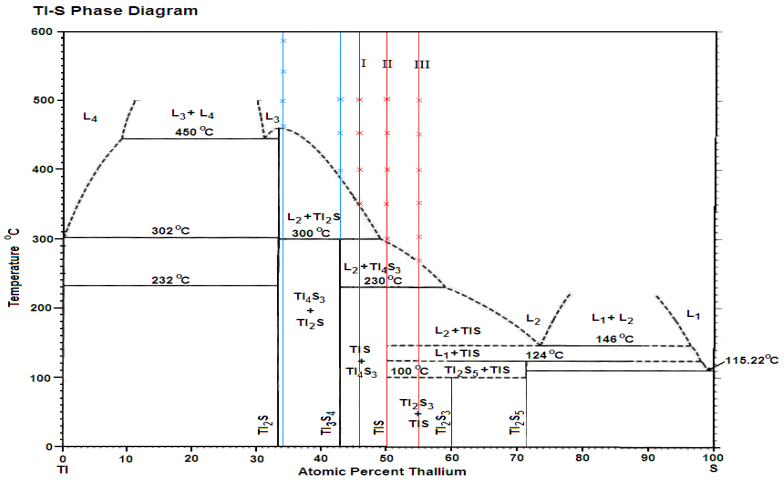

Fig.5 Tl-S phase equilibrium diagram reproduced from Massalski [15] with location of compositions and temperatures at which the thermoelectric power in liquid state was investigated in this paper (alloys I, II, III, marked in red) and in our previous paper [11] (marked in blue)

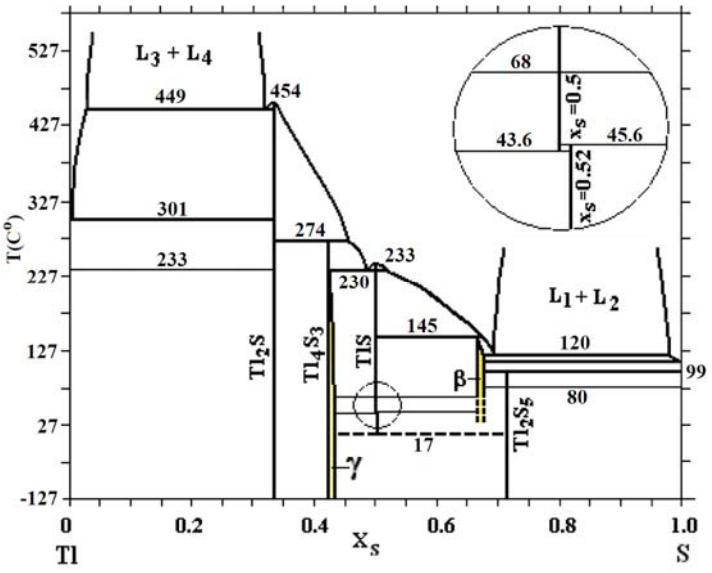

Fig.6 Tl-S phase equilibrium diagram reproduced from Vassiliev [16]

By comparing the two forms of the Tl-S phase diagram (Fig.5 and 6) it appears obvious that in Fig.5 the liquidus line in the region of interest for this paper (30-60at.% S) is higher than in the phase diagram in Fig.6. This remark was crucial for the design of the experiments we have carried out for investigating the

thermoelectric power in liquid state in Tl-S alloys located in the middle of the phase diagram. When selecting the lowest temperature for investigating the thermoelectric power in liquid state an obvious requirement was to make sure that this point was above the liquidus temperature for each alloy and not in the mushy region. Because the details of the phase diagrams and the exact location of the liquidus line are questions still in debate, we have preferred to take into considerations the higher liquidus temperatures as indicated in Fig.5 by Massalski et al., and so to avoid any risk for the lowest investigated points to fall below the liquidus line.

On the other hand the phase equilibrium diagram (Fig.5 and 6) show that all Tl-S alloys for which we have investigated the thermoelectric power in liquid state undergo various phase transformations during heating in view of melting. On this ground we suggest an idea for finding a key to the different behavior of the two groups of alloys (the ones marked in red and the ones marked in blue in Fig.5). This key consists in paying attention to the last crystals to dissolve in the melt or in other words the last crystals that persist up to the liquidus point. These crystals may have a heredidary influence on the microscopic inhomogeneity and the nature of the atomic clusters in the liquid existing in the melt especially in the pre-freezing range. According to the „cluster theory" [17,18] such microscopic inhomogeneity in the melt may influence the energy band structure of the material and consequently its electronic transport properties.

The group of two alloys marked in blue in Fig.5 investigated in our previous paper [11] which exhibited not a dual behavior but a unique semiconductor behavior (decrease of the thermoelectric power when increasing the temperature) were akin to each other. Indeed both alloys consist at room temperature in a mixture of Tl_4S_3 + Tl_2S crystals and both undergo a single phase transformation at 300^{o}C, namely:

$$Tl_4S_3 \rightarrow Tl_2S + L_2$$

As a result of this peritectic reaction in both alloys the last crystals persisting up to the liquidus temperature consisted in Tl_2S (a recognized semiconductor compound both in solid state as well as in liquid state).

Concerning the group of three alloys investigated in the present paper (marked in red as I, II, III in Fig.5) which exhibited a dual behavior of the thermoelectric power in the melt, they differ in their constitution at room temperature. However what really matters is the fact that in all of them the last crystals persisting up to the liquidus temperature consists no more in the semiconductor Tl_2S compound. Instead, according to Fig.6, in alloy I (46 at.%S) the last crystals to dissolve in the melt consist in the Tl_4S_3 compound while in the remaining two alloys, namely alloy II (50 at.%S) and alloy III (55 at.%S) the last crystals to dissolve in the melt consist in the TlS compound.

According to Vassiliev et al.,[16] the evoked compounds undergo various polymorphic transformations and have different crystals structure as presented in Table 4. If one considers the crystal system and the space group for the high temperature polymorph just below the liquidus temperature, one may conclude that each compound may exert a different hereditary influence on the structure of the melt in the pre-freezing region.

Table 4

Crystal structure of thallium –sulfur compounds, reproduced from [16] according to various reference sources

Phase	Space group	Crystal system	a (Å)	b (Å)	c (Å)	Temp-Pression
Tl_2S	R3	Hexagonal	12.12 up to 12.26	-	18.17 up to18.29	25 °C
	HP9	Hexagonal	6.14	-	8.21	above 450°C
Tl_4S_3-α	$P2_1/a$	Monoclinic	7.97	7.757	13.03 γ=103.5°	25°C
β	$P2_1/c$	Monoclinic	7.72	12.982	7.96 γ=104.0°	25°C
TlS	C2	Monoclinic	11.018	11.039	60.16 γ=100.690°	>45.6°C -low
	$P4_12_12$	Tetragonal	7.8039	-	29.552	
	14/mcm	Tetragonal	7.7 up to 7.787	-	6.79 up to6.81	25°C
	R-3mh	Hexagonal	3.945	-	21.788	10 Gpa
	Pm-3m	Cubic	3.2025	-	-	25 GPa
T_2S_5	$R2_12_12_1$	Orthorombic	6.66	6.52	16.75	25°C
T_2S_5	P_{bcn}	Orthorombic	23.45	8.88	10.57	>80°C

To be more specific in the alloys marked in blue in Fig.5 which exhibit an unique semiconductor behaviour in the temperature dependence of the thermoelectric power, the last crystals to dissolve in the melt, namely Tl_2S have a hexagonal structure. In opposition in the alloys marked in red in Fig.5a which exhibit a dual behaviour in the temperature dependence of the thermoelectric power, the last crystals to dissolve in the melt, namely Tl_4S_3 in alloy I and TlS in alloys II and III have a monoclinic structure .

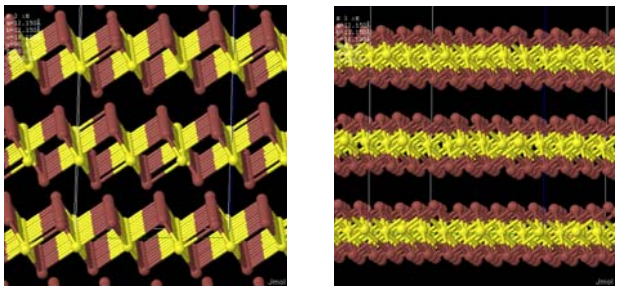

Fig.7 View of the Tl_2S crystal structure

It is interesting to note that what's special with the Tl_2S semiconductor compound is its layer structure (as seen in Fig.7) with strong interatomic bonds within the layers and weak inter-layer bonds. As a result it is not unreasonable to presume that the layered structure of the Tl_2S compound is preserved in the clusters that persist in the melt. This fact is to be ascribed to the preservation of the strong intra-layer bond and the destruction of the weak inter-layer bond. Also expected is a high stability on heating of such clusters because of the strong intra-layer bond.

Moreover some compositional trends become manifest when the experimental data are plotted against the overheating of the melt. To discern such compositional trends we show separately in Fig.8a and Fig.8b the low temperature range where the thermoelectric power of the investigated alloys increases when the temperature increases (Fig.8a) and the high temperature range where the thermoelectric power of the investigated alloys decreases when the temperature increases (Fig.8b). It is easy to see that in the low temperature range (Fig.8a) the investigated alloys range themselves in an ordered sequence, their thermoelectric power increasing as the thallium content increases. In the high temperature range (Fig.8b) the sequence is different, namely the thermoelectric power decreases as the thallium content of the alloy increases.

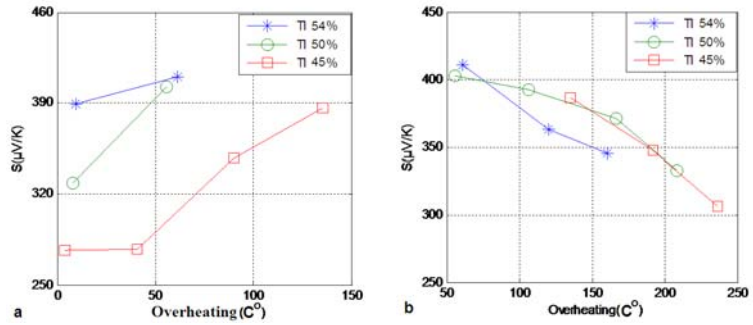

Fig.8 Absolute Seebeck coefficient versus overheating of the melt for the investigated alloys: a.low temperature range; b.high temperature range

Fig.8a also shows that the two alloys which are the poorer in thallium, namely alloy *II* (50 at.%Tl) and and alloy *III* (45 at.%Tl), exhibit a steep slope for the temperature dependence of the thermoelectric power if the Seebeck coefficient is plotted against the overheating of the melt. Even more this slope is seemingly the same for the two alloys. Tentatively we may ascribe this similitude to a common structure of the clusters that may originate from the TlS crystals which are the last to melt in both alloys.

Fig.8a also shows that alloy *I*, which is the richest in thallium (54 at.%Tl) and in which the last crystals that persist up to the liquidus point consist in the Tl_4S_3 compound, exhibits a very gentle slope for the temperature dependence of

the thermoelectric power. One may ascribe this poorly expressed anomalous behaviour of the thermoelectric power in the pre-freezing range to a different structure of the clusters that in this instance have their origin in a different compound, namely Tl_4S_3.

The curves in Fig.8b show that the same disjuncture between alloy *I* on one hand and alloys *II* and *III* on the other hand is also manifest in the high temperature range where the thermoelectric power for all alloys exhibits a semiconductor behavior. Indeed the curves for the temperature dependence of the thermoelectric power appear to be superposed if the Seebeck coefficient for alloys *II* and *III* is plotted against the overheating of the melt, while the curve for alloy *I* appears as distinct.

Finally one may suppose that the differences in the solid state structure indicated by the phase diagram are not completely smeared out when the alloys are melted. Such structural differences in the melt may find an expression in the electronic transport properties as indicated by the results on the thermoelectric power of liquid Tl-S alloys investigated in this paper.

5. Conclusions

A dual behavior in the thermoelectric power temperature dependence has been put in evidence for three liquid alloys located in the middle of the Tl-S phase diagram (54 at.%Tl, 50 at.%Tl and 45at.%Tl). In the high temperature range the behavior was similar to the one obtained in a previous paper for molten Tl-S alloys richer in thallium (57.1 at.%Tl and 64.7 at.%Tl), namely decrease of the Seebeck coefficient as the temperature increases. Such a behavior specific for a one band semiconductor substance is no more observed in the low temperature range encompassing the pre-freezing range where the Seebeck coefficient increases as the temperature increases.

Some interesting compositional influences have been revealed, especially when the temperature dependence of the thermoelectric power was expressed as function of the overheating of the melt above the liquidus point of the alloy.

First, the temperature range in which the special behavior of the thermoelectric power was manifest became broader when the Tl content in the melt decreased, attaining $135^{O}C$ overheating above the liquidus point for the poorest in Tl alloy (45at.%Tl).

Second, the slope of the temperature dependence of the thermoelectric power in the melt was composition dependent and could be put in correlation with the position of the investigated alloy in the phase diagram, or more specifically with the last crystals that persist in its structure up to the liquidus point. For the alloy which was the richest in thallium (54at.%Tl) the last crystals to dissolve in the melt consisted in the Tl_4S_3 compound. For this alloy the slope of the

temperature dependence of the thermoelectric power in the low temperature range was so gentle that one may consider that the special behavior (increase of the thermoelectric power with temperature) was scarcely expressed. In contrast to this, for alloys poorer in thallium (50at.%Tl and 45at.%T) the slope was far steeper and seemingly identical, pointing to an important special behaviour of the thermoelectric power in the pre-freezing range. Since in the latter alloys the last crystals to dissolve in the melt consist in a different compound (TlS) one may ascribe the special behavior of the thermoelectric power in the pre-freezing range to a different nature of the clusters existing in the melt.

R E F E R E N C E S

[1]. Glazov V.M., Chizhevskaya S.N., Glagoleva N.N. Liquid Semiconductors,Plenum Press, New York, 1969
[2]. Tauc J., (ed), Amorphous and Liquid Semiconductors, Plenum Press, New York 1974
[3]. Cutler M., Liquid Semiconductors, Academic Press, New York 1977
[4]. Mott N., Davis E., Electron Processes in Non-Crystalline Materials, Clarendon Press Oxford, 1979
[5]. Nolas G.S., Sharp J., Goldsmid H.J., Thermoelectrics: Basic Principles and New Materials Developments, Springer, New York, 2001
[6]. Yang J., Caillat T., Thermoelectric Materials for Space and Automotive Power Generation Mater.Research Bull., 31 (March), 2006, 224-229
[7]. Venkatasubramanian R., Watkins C., Stokes D., Posthill J., Caylor C., Energy harvesting for electronics with thermoelectric devices using nanoscale materials, Proc. IEEE Intern.Electron Devices Meeting, Washington DC, Dec. 2007, 367-370
[8]. Sales B.C., Critical Overview of Recent Approaches to Improved Thermoelectric Materials, Int.Journal of Applied Ceramic Technology, 4(4), 2007, 291-296
[9]. Xu J., Thermoelectric Properties of Transition Metal Oxides and Thallium Main Group Chalcogenides, Ph D Thesis, University of Waterloo, Ontario, Canada, 2008
[10]. Adam S., Petrescu M.I., Metalurgia International, Special Issue 1, 2013, 77-80
[11]. Adam S., Petrescu M.I., J. Optoelectronics & Advanced Materials, vol.15 (9-10), 2013, 995-1002
[12]. Kusack N., Kendall P., Proc. Phys. Soc.72, 1958, 898
[13]. Nakamura Y., Shimoji M. (1971), Trans.Faraday Soc. 67, 1970, 1270
[14]. Kazandzhan B.I., Tsurikov A.A., (a) Sov. Phys.-Dokl.Phys.Chem. 210, 1973, 430; (b) Russ. J. Phys. Chem. 48, 1974, 429; (c) Russ.J.Phys.Chem.48, 1974, 738; (d) Akad. Nauk SSSR, 48,1974, 746
[15]. Massalski T.B., Okamoto H., Subramanian P.R., Kacprzak L.(editors), Binary Alloys Phase Diagrams, 2nd edition, ASM Publications, USA, 1992
[16]. Vassiliev V.P., Minaev V.S., Tl-S phase diagram , structure and thermodynamic properties, J. Optoelectronics & Advanced Materials, vol.10 (6), 2008, 1299-1305
[17]. Hodginson R.J., J.Phys.C: Solid State Phys., 9, 1976, 1467-1481
[18]. Tsukiya Y., Takeda S., Tamaki S., Waseda Y., Seymour E.F.W., J.Phys.C: Solid State Phys., 15, 1982, 2561-2575